University of Baghdad
College of Engineering
JE
JOURNAL OF ENGINEERING

Journal of Engineering
journal homepage: www.jcoeng.edu.iq
Volume 31 Number 8 August 2025

Assessment of Radiation Risks at the Asalah Site Post-Decontamination Using RESRAD v7.2

Ola Raied Ali [1,*], **Basim Khalaf Rejah** [1], **Murtadha Ahab Sayah** [2]

[1]Department of Physics, College of Science for Women, University of Baghdad, Baghdad, Iraq.
[2]Iraq Atomic Energy Commission, Baghdad, Iraq.

ABSTRACT

Radiation is the emission of energy in the form of particles or photons, and it has two types: cosmic radiation and terrestrial radiation. Materials that emit radiation as they decay over time are called naturally occurring radioactive elements. This study, which was conducted at the Asalah site after removing radioactive contamination, included taking 15 samples from different locations at the site and conducting radiological tests on them using the HpGe (high-purity germanium) system available at the laboratory of Iraqi Atomic Energy Commission- Radiological and Nuclear Applications and Laboratories Directorate From this study one can see that the average value of specific activity for ^{226}Ra was 15.51 Bq/kg, with the highest value for As 9, ranging between 22.2±1.9 Bq/kg and the lowest value for As 2, which was 12±1.4 Bq/kg. The average value (14.56) and the highest value of ^{228}Ac were 25±4.2 Bq/Kg for As 11, while the lowest was 13.5±1.9 Bq/kg for As 12. The average value of ^{40}K was 317.28 Bq/kg, with the highest value (391.6±30.7) Bq/kg in As11 and the lowest value (295±22.3) Bq/kg in As5. The average value for the dose rate was 0.14 µSv/h, ranging from 0.08 µSv/h in As 1 to 0.17 µSv/h. The dose and risk of cancer were elevated using the RESRAD 7.2 code. The external radiation dose at the site decontamination, according to the RESRAD calculations, is 2.5×10^{-7} Sv/year, which is the highest value of any pathway. The total dose from all pathways decreases to 1.1×10^{-7} $Sv/year$. After 100 years, it approaches zero after 1000 years. The total dose determined by RESRAD at the Al-Asalah site is less than the 1 mSv/year acceptable limit for public radiation exposure as established by the IAEA's International Basic Safety Standards.

Keywords: Activity, Analysis, Contamination, Dose, Isotopes, Radiation levels, Risks.

1. INTRODUCTION

Radiation is the emission of energy in the form of particles or waves, playing a crucial role in physics and environmental science. One type of radiation is terrestrial radiation, which comes from naturally occurring radioactive materials, including ^{238}U and ^{226}Ra found within

*Corresponding author
Peer review under the responsibility of University of Baghdad.
https://doi.org/10.31026/j.eng.2025.08.06

Article received: 25/01/2025
Article revised: 16/03/2025
Article accepted: 03/05/2025
Article published: 01/08/2025

the earth **(Najm et al., 2022; UNSCEAR, 2015),** and cosmic radiation originates from space and includes high-energy particles from the sun **(Abdullah, 2018; Mirko et al., 2020).** Radiation is categorized into three types: alpha particles, which are heavy and positively charged; beta particles, which are lighter and may carry a negative or positive charge; and gamma rays, which are uncharged, high-energy electromagnetic waves. **(Kaddoori et al., 2021; IAEA, 2010)**. Natural radioactive elements are isotopes that emit radiation as they decay over time. They play important roles in geology and have significant implications for human health and safety. Natural radioactive elements include ^{238}U, ^{232}Th, and ^{40}K. Uranium mainly exists as ^{238}U, with an average concentration of about 2.8 ppm in the Earth's crust. It has a half-life of approximately 4.468 billion years and a density of 18.95 g/cm^3. Due to its radiotoxicity, ^{238}U is also considered chemically toxic and classified as a metallic element **(Baird et al., 2021).** Research is being conducted to examine uranium ^{238}U concentrations in soil and water because of the impact of its radioactivity on the environment **(Mohammed et al., 2024).** Radiation toxicity indicates the damage that radionuclides can inflict on human health via inhalation or ingestion **(Halstead and Wong, 2025).** The level of harm is influenced by the type and energy of the radiation emitted, with risks arising from both external exposure and internal contamination **(Asia, 2014).** Thorium primarily exists as ^{232}Th, with an approximate concentration of 12 parts per million (ppm) in the Earth's crust. It has a half-life of about 14.05 billion years and a density of 11.72 g/cm^3. While thorium ^{232}Th is less toxic than ^{238}U, it still presents radiological risks and is classified as a metallic element **(Da Conciercao and Bonotto, 2006; Rejah, 2017).** Potassium ^{40}K contains the radioactive isotope ^{40}K, which makes up about 0.012% (120 ppm) of natural potassium. ^{40}K has a half-life of approximately 1.248 billion years and a density of 0.86 g/cm^3. Potassium ^{40}K is classified as a nonmetal; it contributes to natural background radiation and is generally considered to have low toxicity **(Rejah, 2021)**.

These elements are important for comprehending natural processes and their effects on health. Radiation interacts with matter through the processes of ionization and excitation. Ionizing radiation **(Sahani and Dixit, 2022),** including X-rays and gamma rays, transfers energy to electrons, resulting in ionization via mechanisms such as the photoelectric effect, Compton scattering, and pair production **(World Health Organization (WHO), 2023; Cember et al., 2022; Podgorsak, 2020).** Non-ionizing radiation, such as ultraviolet light and microwaves, mainly causes excitation and thermal effects without leading to ionization **(International Atomic Energy Agency, 2024)**. Biologically, radiation can cause DNA damage, including both single-strand and double-strand breaks, which may result in mutations and an increased risk of cancer. Additionally, radiation can lead to cellular effects such as apoptosis and necrosis, impacting tissue health **(ICRP, 2022)**. Radiation exposure can originate from various sources, including natural sources like cosmic rays and radon, medical sources such as imaging and therapy, occupational exposures in certain industries, and the use of radioactive materials in industrial applications **(Jing, 2024; UNSCEAR, 1988).** Understanding these interactions is crucial for risk assessment and safety measures. Radiation pollution remediation is defined as a set of technical processes aimed at reducing or neutralizing radioactive materials in the environment through decontamination and containment, to protect human health and ecosystems **(Padhye et al., 2023)**. These measures are essential for restoring environmental safety and achieving natural balance after contamination resulting from nuclear activities or industrial accidents **(Omoniyi et al., 2023)**. Radiation Pollution Remediation consists of three main methods: Physical Methods involve cleaning surfaces and excavating contaminated soil to remove radioactive materials.

Chemical methods include stabilizing waste to reduce its movement, using solvents to separate radioactive isotopes, and using two methods that combine physical and chemical methods to achieve effective removal of pollutants **(Hang et al., 2024; Claus and Mark, 2016)**.

Using the RESRAD v7.2 code, the dose and risk of cancer were elevated as shown in Figs. 6 and 7. The RESRAD calculations for the site post-decontamination show that the external radiation dose is 2.5×10^{-9} μSv/year, the highest value among all pathways. The total dose from all pathways is $1x10^{-9}$ μSv/year, which decreases to 2×10^{-9} μSv/year after 100 years and approaches zero after 1000 years. It can be compared with the study of **(Basim et al., 2021),** which uses the antioxidation scavenger to reduce the cancer effects on humans.

At the Asalah site, the total dose calculated using RESRAD v7.2 does not exceed the acceptable limit for public radiation exposure, as specified by the International Basic Safety Standards set by the IAEA, which is 1 mSv/year **(Qadr, 2025)**. The cancer risk assessment indicates that the area is considered clean, with calculated values not exceeding acceptable global averages.

The study aims to assess long-term health concerns following decontamination, determine acceptable clearance levels, and evaluate residual radioactivity. By advancing our knowledge of post-remediation environments, this work helps to ensure public safety by facilitating the creation of efficient monitoring plans and preventative measures. To determine whether the site is suitable over living and other human activities, the study intends to measure the amount of remaining organic radioactive substances in the Asalah area in Baghdad-iraq, following the procedure of elimination using an HPGe detector, evaluate dose and cancers risk using a RESRAD v7.2 code, and then contrast its findings with local studies and international standards.

2. MATERIALS AND METHODS

2.1 Sampling and Preparation of Samples (Soil)

Soil samples were collected from the Asalah site in Al-Tuwaitha, approximately 200 km from Baghdad, which covers the area suitable for the study, to evaluate its post-remediation cleanliness. The samples were stored in one-kilogram containers for later analysis. A total of fifteen samples were randomly chosen from different locations within the target area to ensure thorough coverage. Each sample was collected with care to avoid contamination from external sources, then placed in designated containers and securely sealed for transport to the laboratory. The samples were analyzed in the lab to identify contaminants and assess their concentrations in the soil.

To evaluate the level of clearance at the site, fifteen soil samples were collected from the remediation area. Samples were taken from the topsoil at a depth of 0 cm to 5 cm, with each sample weighing approximately 1 kg, and collected using a trowel. After collecting the samples from the site, the first step is to remove gravel or solid materials to isolate the soil, reducing interstitial spaces. The soil is then dried in an oven at a temperature between 80°C and 105°C to prevent the evaporation of radioactive isotopes, such as radon gas, which has a half-life of 3.5 days. The sample is kept at 100°C for at least one hour or until fully dry. Once dried, the soil is passed through a sieve with a 6 mm mesh and mechanically sifted for five minutes to ensure uniform particle size and homogeneity.

The samples were placed in plastic containers for laboratory analysis, and detailed information about each sample, including relevant soil characteristics, was recorded on

adhesive labels attached to the containers. Additionally, the dose rate was measured with an inspector meter from a distance of 1 meter for each sample, and the coordinates and GPS data of the sampling locations were noted, as shown in **Table 1**.
Next, the sample is prepared for weighing. The empty container is weighed and zeroed out. Each sample's unique code is recorded, and the finely ground soil is placed into the container, which is then weighed on a sensitive balance with a precision of four decimal places. The prepared samples are stored for about 30 days to allow radioactive equilibrium to be established, particularly concerning radon gas.

2.2 Gamma Spectroscopy Measurement

The calculation of the net area under the photo peaks in the energy spectrum involved subtracting background counts from the specific peak areas using a HPGe (High Purity Germanium) detector system with Genie 2000 data analysis package in the Iraqi Atomic Energy Commission-Radiological and Nuclear Applications and Laboratories Directorate. This method allowed for the determination of specific activity (Bq/kg) at well-separated high-energy photo peaks **(Hannan, 2024)**. The findings included gamma rays from the progeny of ^{226}Ra in gamma line 609.8 MeV for ^{214}Bi (Bismuth) isotope and ^{228}Ac (Actinium) in the 911.2 MeV gamma line, which exist in secular equilibrium. In addition, ^{40}K was measured directly from its gamma line at 1460 keV. The sample examination time was 3600 seconds **(Alaa and Sura, 2015).**

3. RESRAD CALCULATIONS

A group of workers at the Argonne National Laboratory has developed a set of RESRAD (Residual Radioactivity) codes to analyze the potential radiation exposure of humans and living organisms resulting from environmental contamination by residual radioactive materials. These codes are used to analyze the exposure pathway in the human body and living organisms to assess radiation exposure and the risks resulting from it, and to deduce radiation-free standards and permissible limits for the concentration of radioactive materials in the contaminated environment. In more than 100 countries around the world, RESRAD v7.2 codes are used by universities and organizations interested in assessing radiation risks, which include total dose and risk of cancer.

4. RESULTS AND DISCUSSION

4.1 Gamma Spectroscopy Calculation

Specific Activity (A): Activity in unit mass of the gamma-emitting radionuclides in the sample can be calculated using the following equation (**Jiaying et al., 2022)**:

$$\boldsymbol{A\left(\frac{Bq}{kg}\right) = \frac{N}{I_\gamma \times \varepsilon \times M \times T}} \quad (1)$$

Where A is the specific activity, I_γ is the probability of gamma decay, N is the net count rate of the peak, Ɛ is the detection efficiency, T (3600 sec) is the counting time, and M is the mass of the sample **(Francesca et al., 2025; Rukia, 2023),** as shown in **Table 1**.

Table 1. Explain the sample code, location, ^{226}Ra, ^{228}Ac, ^{40}K, dose rate, and their average values for all studied samples.

No.	Sample Code	Location	^{226}Ra (Bq/kg)	^{228}Ac (Bq/kg)	^{40}K (Bq/kg)	Dose Rate (μSv/h)
1	As 1	N:332155716 E:0445136067	14.5±1.4	18.5 ± 2.2	317 ± 23.8	0.08
2	As 2	N:332157687 E:0445133687	12 ± 1.4	15.5 ± 1.8	297 ± 23	0.15
3	As 3	N:332158437 E:0445131707	14.5 ± 1.3	15.6 ± 1.9	298 ± 23.4	0.13
4	As 4	N:332157387 E:0445129629	14.1 ± 1.6	15.3 ± 2.1	306.3 ± 24	0.16
5	As 5	N:332157421 E:0445129468	17.5 ± 1.5	17.6 ± 1.9	295 ± 22.3	0.16
6	As 6	N:332152837 E:0445130782	14.8 ± 1.6	15 ± 2.2	271 ± 23	0.11
7	As 7	N:332159202 E:0445155294	13.4 ± 1.4	18 ± 2	310.6 ± 24	0.16
8	As 8	N: 332168295 E: 445138622	17.5 ± 1.6	20.5 ± 2.4	338.3 ± 25.5	0.17
9	As 9	N:332145758 E:0445123401	22.2 ± 1.9	16 ± 2.1	359 ± 25.8	0.16
10	As 10	N:332154963 E:0445116974	15 ± 1.7	21 ± 2.5	324.3 ± 26	0.15
11	As 11	N:332133586 E:0445103215	15.5 ± 1.8	25 ± 4.2	391.6 ± 30.7	0.16
12	As 12	N:337170286 E:0445194162	15.4 ± 1.5	13.5 ± 1.9	291.2 ± 23.2	0.15
13	As 13	N:3313123 E:04431315	15.7 ± 1.6	20.4 ± 2.1	338.4 ± 25	0.13
14	As 14	N:3312554 E:04432419	17.5 ± 1.8	14.8 ± 2.3	289.6 ± 25.3	0.13
15	As 15	N:3312239 E:04433030	13.1 ± 1.4	16.7 ± 1.9	332 ± 25	0.12
	Average		15.51	17.56	317.28	0.14

From **Table 1**, one can note that the average value of specific activity for ^{226}Ra was 15.51Bq/kg, with the highest value ranging between (22.2±1.9) Bq/kg for as 9 and the lowest value in As 2, which was (12±1.4) Bq/kg as shown in **Fig.1.** For ^{228}Ac, the highest value was (25± 4.2) Bq/kg for As 11, while the lowest value was (13.5± 1.9) Bq/kg for As 12 as shown in **Fig. 2**. Regarding ^{40}K, the highest value was (391.6±30.7) Bq/kg in sample 11, and the lowest value was (295± 22.3) Bq/kg in sample 5 with the average value was 317.28 Bq/kg as shown in **Fig. 3**. **Fig. 4** shows that the average dose rate was 0.14 μSv/h, ranging from 0.08 μSv/h for As 1 to 0.17 μSv/h in As 8. In contrast, **(Basim et al., 2021)** this study focused on characterizing contaminated areas at the AL-Nahrawan site using portable Geiger-Müller devices and scintillation detectors. Surface contamination ranged from 0.46 to 50.9 Bq/cm^2, with radiation exposure levels between 0.016 and 1.823 mRad/hr. The activity concentrations of radionuclides in soil samples exceeded accepted limits, indicating contamination above background levels. The study highlighted an elevated cancer risk

(2.2×10^{-3}) at this site, compared to the global average reported by UNSCEAR (0.29×10^{-3} to 1.16×10^{-3}). Restrictions on public use of the site are recommended.

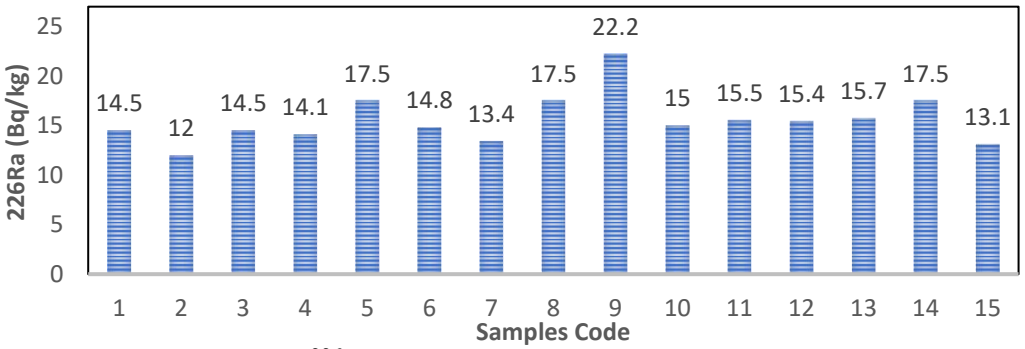

Figure 1. ^{226}Ra concentration in all studied samples.

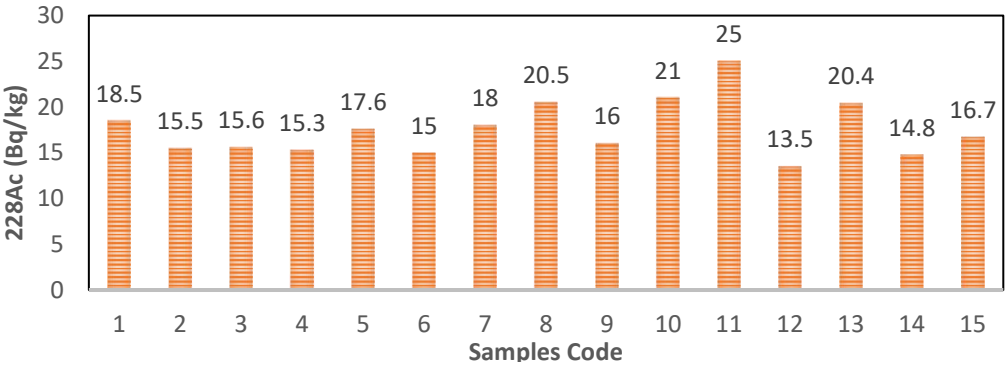

Figure 2. ^{228}Ac concentration in all studied samples.

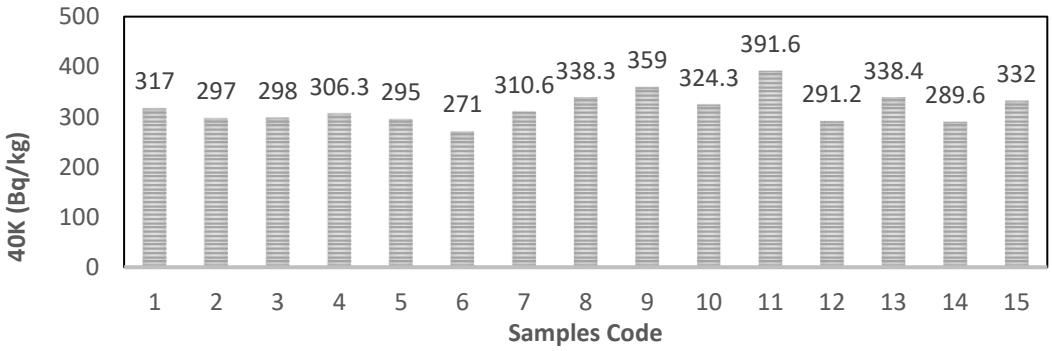

Figure 3. ^{40}K concentration in all studied samples.

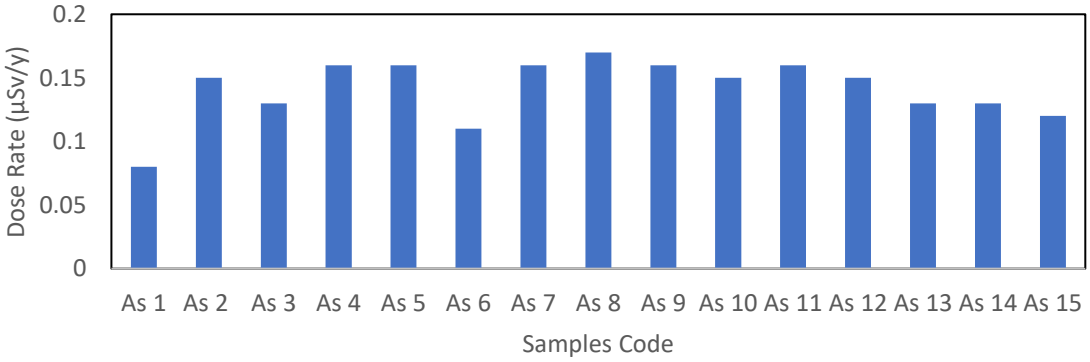

Figure 4. The dose rate in all samples.

4.1.1 Descriptive Statistics

Table 2 shows that potassium has a high concentration (391.6 Bq/kg), nearly twice that of radium and actinium so the coefficient of variation (that represents the average of the squared differences from the mean value) will have a high value (960.766%), as this value is believed to indicate that the high concentration in the studied region comparing with that values of variance Ra and Ac (6.004, 9.428))%, respectively. While the measure of how spread-out numbers are, the standard deviation confirms this result.

Table 2. Descriptive Statistics of the measurement results.

Element	No. of Samples	Minimum	Maximum	Mean	Std. Deviation
Ra	15	12.00	22.20	15.5133	2.45033
Ac	15	13.50	25.00	17.5600	3.07055
K	15	271.00	391.60	317.2867	30.99622
D	15	0.08	0.17	0.1413	0.02446
Average		74.145	109.74	87.62	9.135

4.1.2 Frequentist probability

Probability is the likelihood that an event will transpire within a specific set of probable results. It is a useful and quick way of distributing measured values. **Figs. 5 to 8** show the concentrations of Ra, Ac, K, and D, respectively, for all samples. From this study, one can observe an expected calculated normal distribution (bell-shaped) with a single peak (black curve) and a gradual decrease (taper) at both ends of the figure. It can also be seen from the figure that there is an approximate symmetry of the two sides of the distribution (the highest and lowest values for each variable), where each one has an unequal population in a certain parameter. This data and the following figures were obtained using the IBM SPSS statistical program.

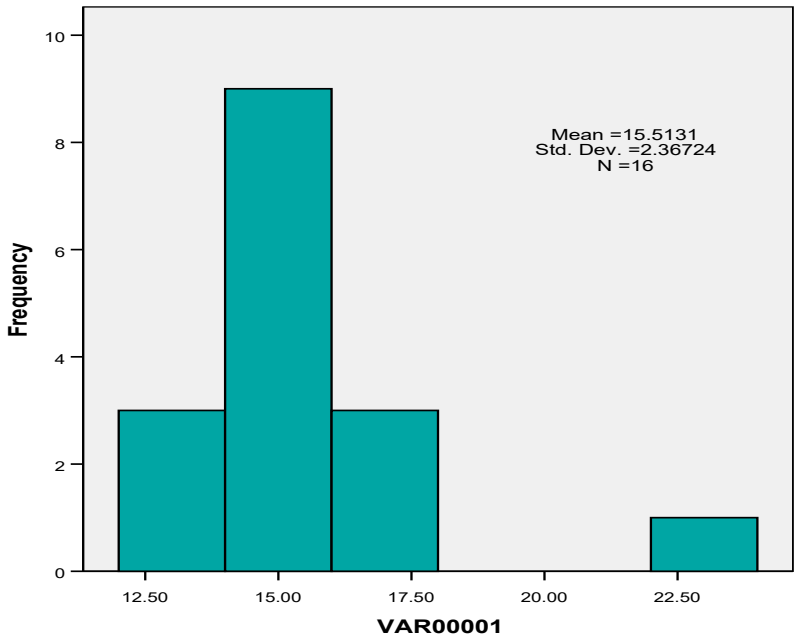

Figure 5. Represent the frequency distribution of the concentration of the measurement values for Ra-226.

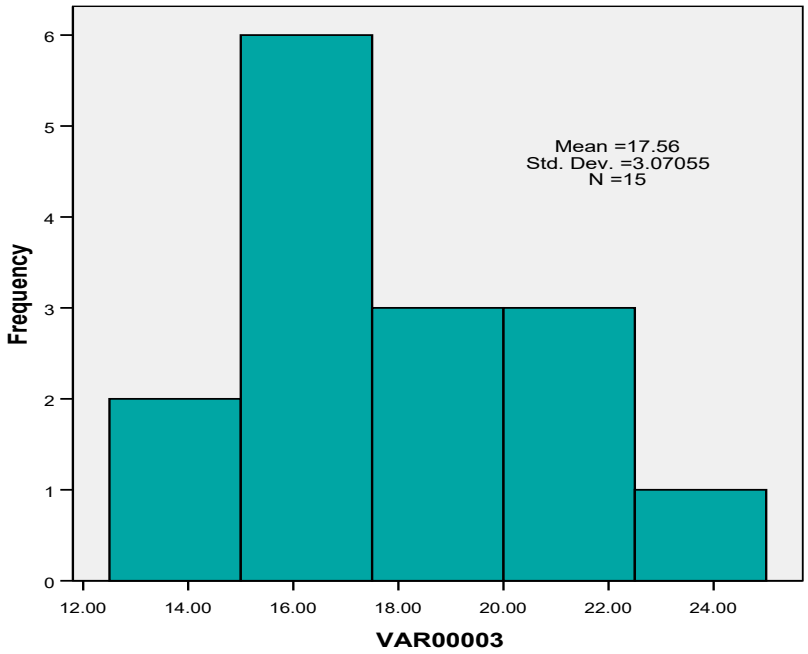

Figure 6. Represent the frequency distribution of the concentration of the measurement values for Ac-228.

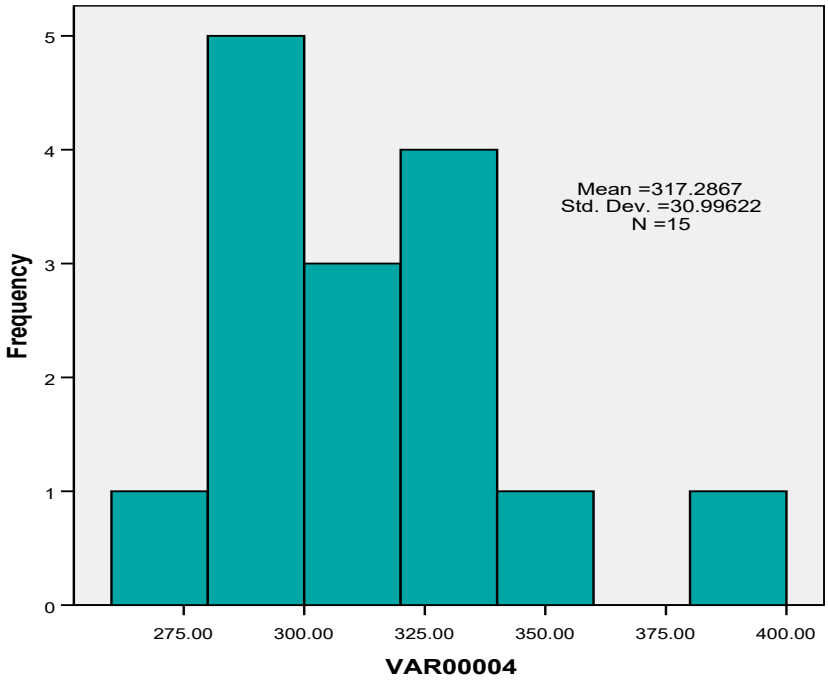

Figure 7. Represent the frequency distribution of the concentration of the measurement values for K-40.

4.1.3 RESRAD calculation

From the risk cancer assessment calculated using RESRAD, the area is considered clean, and the cancer risk is negligible as the calculated values do not exceed the acceptable global average values according to the UNSCEAR (United Nations Scientific Committee on the Effects of Atomic Radiation) **(UNSCEAR, 2000).** which specifies that the acceptable limit for public exposure is not to exceed 1 mSv/year, as shown in **Figs. 9 and 10**.

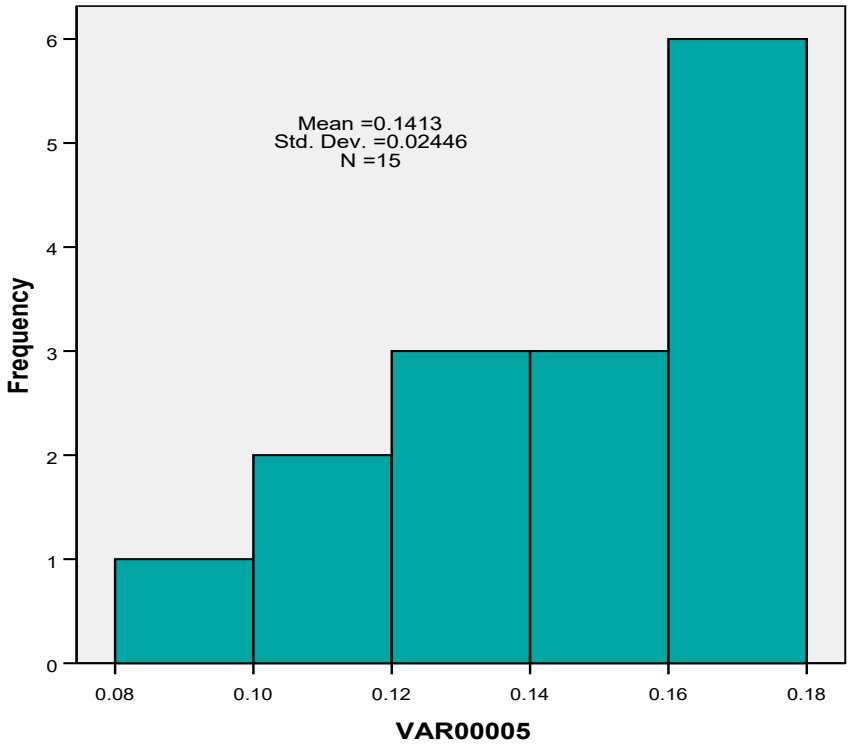

Figure 8. Represent the frequency distribution of the dose rate of the measurement values.

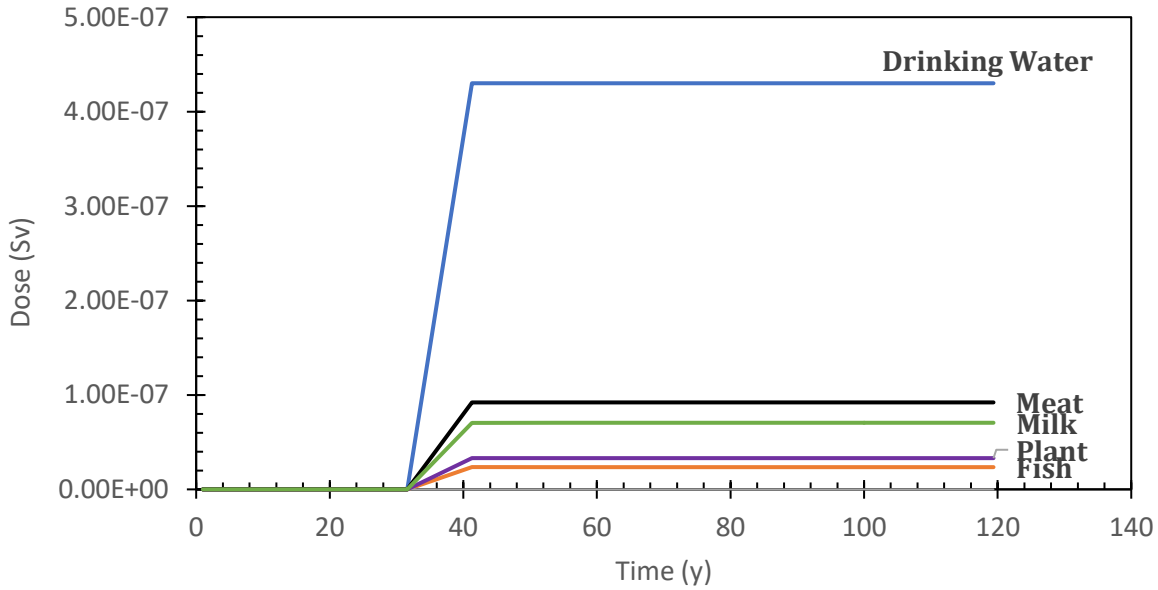

Figure 9. Explain the dose in all nuclides summed and component pathways.

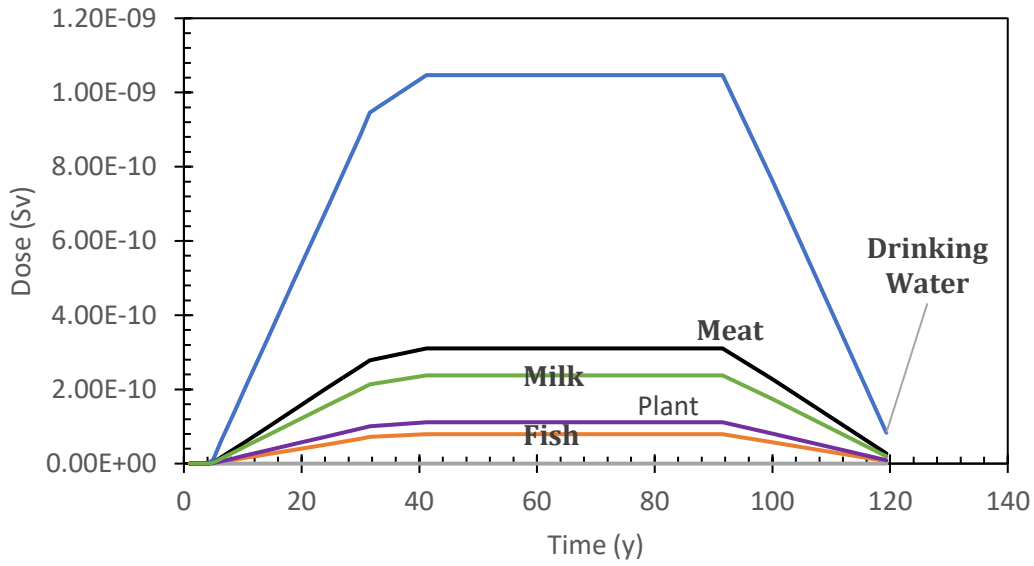

Figure 10. Explain the excess cancer risk in all nuclides summed and component pathways.

5. CONCLUSIONS

Laboratory analysis using an HPGe detector on samples from the site confirmed that radiation doses at the Asalah site do not exceed the average levels found in clean areas. The concentrations of ^{226}Ra, ^{232}Th, and ^{40}K in the soil samples are lower compared to international standards and neighboring regions, making it suitable for human activities. Random measurements at various points on the site revealed that radiation levels are within acceptable limits for public exposure according to IAEA (International Atomic Energy Agency) standards. The calculations show that the concentrations of radioactive elements fall within acceptable international limits, confirming the suitability of the site for habitation. The results of this study, which were obtained using the RESRAD 7.2 code, showed that the calculated dose falls within the permissible limit in the international safety standards set by the International Atomic Energy Agency, which is 1 mSv/year. As a result, the site is now safe for habitation. The results of the soil sample testing were below the allowable level because there was no radiation present. Residential development, commercial project establishment, agricultural usage, and industrial use are among the suggested applications for a protected location in the Al-Tuwitha region, for the Al-Asala site.

NOMENUCLATURE

Symbol	Description	Symbol	Description
A	Specific activity	**Ɛ**	Detection efficiency
N	Net count rate of the peak	**T**	Counting Time(3600sec)
Iγ	Probability of gamma decay	**M**	Mass of the sample
A	Area	**yr**	Year
Bq	Becquerel	**hr.**	Hours
Sv	Sievert	**g**	Gram
ppm	Parts per million	**Kev**	Kilo electron volt

Credit Authorship Contribution Statement

Ola Raied Ali made significant contributions to the literature review of the research and the collection of necessary samples, in addition to carrying out the practical aspect and its application. Murtadha Adhab Sayah performed the meticulous data analysis and interpretation of the results. Basim Khalaf Rejah was responsible for drafting and revising the final manuscript.

Declaration of Competing Interest

The authors declare that they have no known competing financial interests or personal relationships that could have appeared to influence the work reported in this paper.

REFRENECE

Abdullah A. M. A. 2018. Increasing awareness of radiation hazards and radiation protection among medical staff. *Acta Scientia rum. Health Sciences*, 45, e59256.

Alaa, B. K., and Sura, S. F., 2015. Calculation of full energy peak efficiency for HPGe detector using the Monte Carlo method. *Iraqi Journal of Science*, vol. 56(4B), pp. 3246-3255. https://ijs.uobaghdad.edu.iq/index.php/eijs/article/view/9432

Al-Mashhadani, A., 2014. Characterization and classification of radioactive wastes from disposal soil. *Iraqi Journal of Science*, 55(2), pp. 741-749. https://ijs.uobaghdad.edu.iq/index.php/eijs/article/view/11791

Baird, C., and Cann, M., 2021. *Environmental chemistry. 5th ed*. New York: W. H. Freeman. https://www.amazon.com/Environmental-Chemistry-Colin-Baird/dp/1429277041

Baker, J. A., and Murphy, M. 2022. Techniques for remediation of radioactive contamination in soil and water. *Journal of Environmental Management*, 301, P. 113750.

Basim, H. E., Murtdha, A., Asia H. A. 2021. Risk assessment for the Al-Nahrwan site that is contaminated with depleted uranium in Baghdad. *Journal of Chemical Health Risk*, 11(3), pp. 317-328. https://jchr.org/index.php/JCHR/article/view/135

Cember, H., Johnson, T. 2022. *Introduction to health physics. 5th ed*. New York: McGraw-Hill.

Claus G. and Mark R., 2016. Radioactivity and radiation. *Springer International Publishing Switzerland*. https://doi.org/10.1007/978-3-319-42330-2.

Da Conceicao F.T., and Bonotto D.M., 2006. Radionuclides, heavy metals, and fluorine incidence at Tapira phosphate rocks, Brazil, and their industrial products. *Environmental Pollution*.139(2), pp. 232-243. http://dx.doi.org/10.1016/j.envpol.2005.05.014.

Francesca F., Pier P., Giovanna M., Nicola Z., Mickael P., Veronique M., Olivier D., Laurence L., Gianpiero A., Marcella M., Elena P. and Matteo C., 2025. Skin absorption of metals derived from hydrogenated stainless particles in human skin: Results from the TITANS Project. *Environmental Pollution*, 364, P. 125327. https://doi.org/10.1016/j.envpol.2024.125327.

Hang Y., Qi F., Weixiang X., yadong T., Guoliang B., yunli L., Zisen L., Shibin X., Zhenbin W., and Yi Z., 2024. Unraveling the nuclear isotope tapestry: application, challenges, and future horizons in a

dynamic landscape. *Eco-Environment & Health,* 3(2), pp. 208-226. https://doi.org/10.1016/j.eehl.2024.01.001

Hannan Y., Mohammed A., Umair A., Mohammed Sh., Abdulrahman Al., Baji Sh., Antalov J., Shawn J., and Muhammed A., 2024. Comprehensive analysis of contaminants in powdered milk samples using an HPGe for gamma radiation. *ACS Omega Journal.* 9(19). https://doi.org/10.1021/acsomega.4c00648

ICRP, 2022. Radiation detriment calculation methodology. ICRP Publication 152. Ann. ICRP, 51(3). https://www.icrp.org/publication.asp?id=ICRP%20Publication%20152

International Atomic Energy Agency (IAEA), 1995. The principles of radioactive waste management (Safety Fundamentals). Safety Series. No. 111-F. IAEA, Vienna.

International Atomic Energy Agency (IAEA), 2010. Governmental, legal, and regulatory framework for safety. IAEA Safety Standards Series No. GSR Part 1, IAEA, Vienna. https://www-pub.iaea.org/MTCD/Publications/PDF/Pub1713web-70795870.pdf

International Atomic Energy Agency (IAEA), 2024. radiation safety in the use of radiation sources in research and education. IAEA Safety Standards Series No. SSG-87, Vienna. https://doi.org/10.61092/iaea.0f4a-dm2n.

Jiaying W., Yu Ch., Zhongjian M., Luz H., and Zhen Z., 2022. Analysis of gamma-emitting radionuclides in soils around high-energy accelerators. *Radiation Medicine and Protection,* 3(4), pp. 171–174. https://doi.org/10.1016/j.radmp.2022.10.004

Jing C. 2024. A summary of the UNSCEAR evaluation on medical exposure to ionizing radiation and a call for more representative data. *Radiation Medicine and Protection*, 5(1), pp. 7-10. https://doi.org/10.1016/j.radmp.2023.12.001

Kaddoori, F., Rejah, B., and Fzaa, W., 2021. Measuring the pollution level with uranium and radon in the soil of some areas inside the Baghdad University Campus-Al-Jadiriyah. *NeuroQuantology*, 19(7), pp. 72–77.

Lokesh P., Prashant S., Tahereh J., Shiv B., Deyi H., Sabry Sh., Jörg R., David O'., Dane L., Hailong W., Kadambot S., and Nanthi B., 2023. Contaminant containment for sustainable remediation of persistent contaminants in soil and groundwater. *Journal of Hazardous Materials,* 445(5), P. 131575. https://doi.org/10.1016/j.jhazmat.2023.131575.

Mirko B., Riccardo M., and Piergiorgio P., 2020. Cosmic ray detection in space. *Progress in Particle and Nuclear Physics*. 112, P. 103765. https://doi.org/10.1016/j.ppnp.2020.103765.

Mohammed M., Akram A., Mazin A., Duha K., and Muslim A., 2024. Developing a Copper-Zinc-Aluminum alloying technique by vacuum thermal deposition after irradiation by Gamma rays (Nai (Ti) with stabilized Zinc metal. Vacuum. 219A, P. 112676. https://doi.org/10.1016/j.vacuum.2023.112676.

Najm M., Rejah B., and Husseini H., 2022. NORM and hazard indices in soil and dates of palm groves in Baghdad governorate, Iraq. *Physica Scripta*, 97(9), P. 095305. http://doi.org/10.1088/1402-4896/ac8703.

Omoniyi K., Oluwaferanmi O., and Adeyemi O., 2023. Environmental and ecological impact of radioactive waste disposal. *World Journal of Advanced Research and Reviews,* 18(02), pp. 1419-1439.

Podgorsak B. 2016. *Radiation physics for medical physicists. 2nd ed*. New York: Springer.

Qadr, H.M., 2025. Radon, Radium, Polonium, and Uranium concentrations in the rocks determined by passive method in Kurdistan Region, Iraq. *Environmental Forensics*, pp. 1-11. https://doi.org/10.1080/15275922.2025.2490472.

Rejah B., 2017. Specific activities of natural radionuclides and annual effective dose due to the intake of some types of powdered milk available in Baghdad markets. *Baghdad Science Journal*, 14(3), pp. 619–624. https://doi.org/10.21123/bsj.2017.14.3.0619.

Rejah B., Kaddoori F., Hamza S.S., and Wadi S., 2021. Measurement of specific activity of natural radioactive materials and cs-137 in soil samples for some areas in Al-Doura City in Baghdad Governorate. *Iraqi Journal of Science*, 62(9), pp. 2940–2947. https://ijs.uobaghdad.edu.iq/index.php/eijs/article/view/3130

Rukia J., Ali H., and Ali A., 2023. Estimation of natural radioactivity in the soil of primary schools in the old city of Najaf. *Arab Journal of Nuclear Science and Application*, 56(1), pp. 117-125.

Sahani R., and Ambesh D., 2022. A comprehensive review of Zinc Oxide bulk and nano-structured materials for ionizing radiation detection and measurement applications. *Materials Science in Semiconductor Processing*, 151(15), P. 107040. https://doi.org/10.1016/j.mssp.2022.107040

United Nations Scientific Committee on the Effects of Atomic Radiation (UNSCEAR), 1988. *Sources, effects and risks of ionizing radiation*. New York (USA) https://www.unscear.org/unscear/publications/2020_2021_1.html

UNSCEAR–United Nations Scientific Committee (UNSCEAR), 2000. The Effects of Atomic Radiation: Sources and Effects of Ionizing Radiation. *Report to General Assembly, with Scientific Annexes*.

World Health Organization (WHO), 2023. Ionizing Radiation, Health Effects. https://www.who.int/news-room/fact-sheets/detail/ionizing-radiation-and-health-effects

تقييم مخاطر الاشعاع في موقع الاسالة بعد إزالة التلوث باستخدام برنامج ريسارد الإصدار 7.2

علا رائد علي[*,1] , باسم خلف رجه[1] , مرتضى عذاب صياح[2]

[1]قسم الفيزياء , كلية العلوم للبنات , جامعة بغداد , بغداد ، العراق
[2]هيئة الطاقة الذرية العراقية، بغداد ، العراق

الخلاصة

الإشعاع هو انبعاث الطاقة على شكل جسيمات أو فوتونات، وله نوعان: الإشعاع الكوني والإشعاع الأرضي. وتُسمى المواد التي تُصدر إشعاعًا أثناء تحللها بمرور الوقت العناصر المشعة الطبيعية. تضمنت هذه الدراسة، التي أُجريت في موقع الأصالة بعد إزالة التلوث الإشعاعي، أخذ 15 عينة من مواقع مختلفة في الموقع وإجراء اختبارات إشعاعية عليها باستخدام منظومة HpGe (الجرمانيوم عالي النقاء) والمتوفر في مختبر هيئة الطاقة الذرية العراقية – مديرية التطبيقات والمختبرات الإشعاعية والنووية. من خلال هذه الدراسة، يمكن ملاحظة أن المعدل الوسطي للنشاط النوعي لنظير Ra–226 بلغ 15.51 بيكريل/كغ، حيث سُجلت أعلى قيمة في العينة As9 وكانت 22.2 ± 1.9 بيكريل/كغ، بينما كانت أقل قيمة في العينة As2 وقد بلغت 12 ± 1.4 بيكريل/كغ. أما المعدل الوسطي لنظير Ac–228 فقد بلغ 14.56 بيكريل/كغ، وسُجلت أعلى قيمة عند 25 ± 4.2 بيكريل/كغ، وأقل قيمة كانت 0.3 ± 1.9 بيكريل/كغ في العينة As12. فيما يخص نظير K–40، بلغ المتوسط 317.28 بيكريل/كغ، وسُجلت أعلى قيمة في العينة As11 بمقدار 391.6 ± 30.7 بيكريل/كغ، وأقل قيمة في العينة As5 بمقدار 295 ± 22.3 بيكريل/كغ. أما معدل الجرعة الإشعاعية فقد بلغ متوسطه 0.14 ميكروسيفرت/ساعة، حيث تراوح بين 0.08 في العينة As1 و0.17 ميكروسيفرت/ساعة. تم احتساب الجرعة ومخاطر الإصابة بالسرطان باستخدام برنامج RESRAD 7.2. وقد أظهرت حسابات RESRAD أن أعلى قيمة للجرعة الإشعاعية الخارجية في موقع التطهير بلغت 2.5×10^{-9} ميكروسيفرت/سنة، وهي الأعلى بين جميع المسارات المحتملة. كما أن الجرعة الكلية من جميع المسارات انخفضت إلى 1.1×10^{-9} ميكروسيفرت/سنة. وبعد مرور 100 عام تقترب هذه القيمة من الصفر، وتصل إلى الصفر تقريبًا بعد 1000 عام.وقد تبين أن الجرعة الكلية التي حددها برنامج RESRAD في موقع الأصالة أقل من الحد المقبول البالغ 1 ميلي سيفرت/سنة للتعرض الإشعاعي العام، كما حددته المعايير الأساسية الدولية للسلامة الصادرة عن الوكالة الدولية للطاقة الذرية (IAEA).

الكلمات المفتاحية: النشاط، التحليل، التلوث، الجرعة، النظائر، مستويات الاشعاع، المخاطر.